

Cell Metabolism, Volume 12

Supplemental Information

PERILIPIN-Dependent Control of Lipid Droplet

Structure and Fat Storage in *Drosophila*

Mathias Beller, Anna V. Bulankina, He-Hsuan Hsiao, Henning Urlaub, Herbert Jäckle, and Ronald P. Kühnlein

Supplemental Experimental Procedures

Fly techniques

If not stated otherwise flies were propagated on a complex cornflour-soyflour-molasses food (cornflour and barley malt 80g/l each, molasses 22g/l, yeast 18g/l, soyflour 10g/l, agar-agar 8g/l, propionic acid 6.3ml/l and nipagin 1.5g/l), supplemented with dry yeast at 25°C and 20-30% humidity with a 12h/12h light/dark cycle.

plin1 mutant clones were generated using the stocks RKF1036-38 (see comprehensive fly stock table; supplemental experimental procedures). Heterozygous *plin1*⁻ embryos 0-8 hours of age were heat shocked for 20 minutes at 38°C and mutant clones in the fat body were analyzed at migratory L3 larval stage.

For the *plin1* genomic rescue transgene construct sequences representing chromosome 3R positions 19589032 to 19592544 (*D. melanogaster* genome assembly release 5.5) were PCR-amplified and subcloned to pCaSpeR4 (Note that the *plin1* genomic rescue transgene encodes the following amino acid substitutions compared to the annotated PLIN1-PC isoform: pos. 238 P->H and pos. 337 L->P).

The PLIN1 and PLIN1^{ΔH} effector transgenes were constructed by cloning the wild type or the hexa-mutated (Stratagene QuikChange Lightning Site Directed Mutagenesis kit) PLIN1-PC open reading frame into pUASTattB (Bischof et al., 2007). The phiC31 transgenesis system (Bischof et al., 2007) was employed to ensure comparable expression levels of PLIN1 and PLIN1^{ΔH} in the adipose tissue of *plin1* mutant flies. Note that the C-terminus of PLIN1 and PLIN1^{ΔH} differs from the annotated PLIN1-PC sequence (CSRRYL as compared to GVV).

A *plin1* RNAi snapback transgene was constructed by sequential cloning of fragments from *plin1* cDNA GH10767 (DGRC; <https://dgrc.cgb.indiana.edu>) representing pos. 437-858 and 440-856 of *plin1*-RC (www.flybase.bio.indiana.edu) into pUASTIhp. The *plin1* cDNA rescue effector construct was generated by cloning a 1.3kbp *EcoR1* fragment of GH10767 covering the PLIN1-PC open reading frame (plus 48bp 5'UTR and 13bp 3'UTR) into pUAST. For the *plin1::EGFP* effector transgene, the PLIN1-PC open

reading frame was cloned into pEGFP-N2 (www.clontech.com) and the *plin1::EGFP* fusion gene subcloned into pUAST. The *HsPLIN1* effector transgene was derived from IMAGp998M1111718 (www.imagenes-bio.de) and sequences from -16 to +112 relative to the *HsPLIN1* open reading frame were cloned into pUAST. All cDNA-based transgenes were expressed under control of the UAS/Gal4 system (Brand and Perrimon, 1993). More details on all transgene constructs are provided on request.

PKAc overexpression selectively in the adult fly fat body was achieved using the TARGET system (Kiger et al., 1999; McGuire et al., 2003).

Transgenic fly stocks were established by P-element-mediated germ line transformation in a w^{1118} strain or the stock RKF1014.

Fly stocks

The following fly stocks were used in this study:

Short name	Stock number	Genotype	Reference/ source
<i>plin1</i> ^{G4304}	RKF611	w^* ; <i>plin1</i> ^{G4304} / TM3, <i>ry</i> ^{RK} <i>Sb</i> ¹ float	GenExel Inc.
<i>plin1</i> ^{rev} (<i>plin</i> ⁺)	RKF676	w^* ; <i>plin1</i> ^{rev}	this study
<i>plin1</i> ¹ (<i>plin</i> ⁻)	RKF649	w^* ; <i>plin1</i> ¹	this study
<i>plin1</i> ²	RKF650	w^* ; <i>plin1</i> ² / TM3, <i>Sb</i> ¹	this study
<i>bmm</i> ⁻	SGF529	w^* ; <i>bmm</i> ¹ / TM3, <i>Sb</i> ¹ float.	(Grönke et al., 2005)
<i>mdy</i> ⁻	RKF1004	w^* ; <i>mdy</i> ^{QX25} <i>cn</i> ¹ <i>bw</i> ¹ / CyO float	(Buszczak et al., 2002)
<i>plin1::EGFP</i> (effector)	RKF587	w^* ; P{ w^{+mC} UAS- <i>plin1::EGFP</i> } / TM3 <i>Sb</i> ¹ <i>e</i> ¹	this study
<i>Df(3R)mbc-30</i>	RKF553	<i>cn</i> ¹ ; <i>Df(3R)mbc-30</i> / TM3, <i>Sb</i> ¹	BDSC #4940
<i>plin1</i> RNAi (effector)	RKF554	w^* ; P{ w^{+mC} UAST <i>Ihp plin1</i> } / CyO- <i>hb-beta-gal</i>	this study
conditional <i>plin1</i> RNAi (effector)	RKF1001	w^* ; P{ w^{+mC} UAST <i>Ihp plin1</i> } / CyO; P{ $w[+mC]=tubP-Gal80^{ts}$ } / TM6C, <i>Sb</i> ¹ <i>Tb</i> ¹ float	this study
<i>plin1</i> genomic rescue	RKF678	w^* P{ <i>CaSpeR4 plin1</i> }; +/+; <i>plin1</i> ¹	this study
<i>plin1</i> cDNA rescue (effector)	RKF680	<i>y</i> [*] float w^* ; P{UAST <i>plin1</i> } / CyO float; <i>plin1</i> ¹ / TM3 <i>Sb</i> ¹ <i>e</i> ¹ float	this study
conditional <i>plin1</i> cDNA rescue (effector)	RKF1006	w^* ; P{ w^{+mC} UAS- <i>plin1</i> }; P{ $w[+mC]=tubP-Gal80^{ts}$ } <i>plin1</i> ¹	this study
fat body driver	RKF125	w^* ; P{ $w[+mW.hs]=GawB$ }FB+SNS	(Grönke et al.,

			2003)
fat body driver <i>UAS-GFP</i>	RKF153	$y^* w^*$; $P\{w[+mW.hs]=GawB\}FB$ $P\{w^{+m*} UAS-GFP 1010T2\}$; +/+	(Grönke et al., 2003)
fat body driver <i>plin1⁻</i>	RKF910	w^* ; $P\{w^{+mW.hs}=GawB\}FB+SNS / CyO$ <i>float.</i> ; <i>plin1¹/TM6C, Sb¹Tb¹ float.</i>	this study
fat body driver <i>UAS-GFP</i> <i>plin1⁻</i>	RKF682	$y^* float w^*$; $P\{w^{+mW.hs}=GawB\}FB$ $P\{w^{+m*} UAS-GFP 1010T2\}\#2 / CyO$ <i>float; plin1¹/ TM3 Sb¹ e¹ float</i>	this study
conditional fat body driver <i>UAS-GFP</i>	RKF805	$y^* w^*$; $P\{w^{+mW.hs}=GawB\}FB P\{w^{+m*}$ $UAS-GFP 1010T2\}\#2$; $P\{w^{+mC}=tubP-GAL80^{ts}\}2$	this study
conditional fat body driver <i>UAS-GFP</i> <i>plin1⁻</i>	RKF1009	$y^* float w^*$; $P\{w^{+mW.hs}=GawB\}FB$ $P\{w^{+m*} UAS-GFP 1010T2\}$; $P\{w^{+mC}=tubP-Gal80^{ts}\}7 plin1^1$	this study
<i>ptc</i> driver	RKF123	w^* ; $P\{w^{+m*} ptc-Gal4\}$	(Vorbrüggen and Jäckle, 1997)
<i>plin2</i> RNAi (effector)	RKF1151	w^{1118} ; $P\{GD14108\}v40734$	(Dietzl et al., 2007)
<i>AKHR⁻</i>	RKF639	$y^* float w^*$; <i>AKHR¹/ CyO float</i>	(Grönke et al., 2007)
<i>bmm⁻ plin1⁻</i>	SGF766	w^* ; <i>bmm¹, plin1¹/ TM3 Sb¹e¹ float</i>	this study
<i>AKHR⁻ plin1⁻</i>	RKF752	w^* ; <i>AKHR¹/ CyO-ftz-lacZ float; plin1¹</i> <i>/ TM3-ftz-lacZ Sb¹ ry* float</i>	this study
<i>plin1⁻ bmm</i> effector	RKF702	$y^* float w^*$; $P\{w^{+mC}$ $bmm^{ScerUAS}=UAS-bmm\}\#2c / CyO-$ <i>ftz-lacZ float ; plin1¹/ TM3 Sb¹ ry*</i> <i>float</i>	this study
<i>bmm</i> effector	SGF532	w^* ; $P\{w^{+mC} bmm^{ScerUAS}=UAS-$ $bmm\}\#2c$; +/+	(Grönke et al., 2005)
<i>PKAc</i> effector	RKF720	w^* ; <i>UAS-PKAc</i> ; +/+	(Kiger et al., 1999)
<i>plin1⁻ PKAc</i> effector	RKF767	w^* ; <i>UAS-PKAc; plin1¹</i>	this study
<i>plin1⁻ PLIN1^{ΔH}</i> effector	RKF1097	w^* ; +/+; $P\{UAST PLIN1-PC S8A$ $S20A, S124A, T206A, S253A,$ $S277A\}at 86Fb plin1^1 / TM3, Sb^1 e^1$ <i>float</i>	this study
<i>plin1⁻ PLIN1</i> effector	RKF1020	w^* ; +/+; $P\{UAST PLIN1-PC\}at 86Fb$ $\#3A plin1^1 / TM3, Sb^1 e^1 float.$	this study
<i>mdy⁻ plin1⁻</i>	RKF779	w^* ; $mdy^{QX25} cn^1 bw^1 / CyO, P\{w^{+mC}$ $=ActGFP\}JMR1 float; plin1^1$	this study
<i>mdy⁻ bmm⁻</i>	RKF780	w^* ; $mdy^{QX25} cn^1 bw^1 CyO, P\{w^{+mC}$	this study

		<i>ActGFP</i> }JMR1 float; <i>bmm</i> ¹ /TM3, P{w ^{+mC} <i>ActGFP</i> }JMR2, <i>Ser</i> ¹ float	
	RKF1036	<i>w</i> [*] ; P{ry ^{+t7.2} =neoFRT}82B P{w ^{+mC} =Ubi-GFP}	Alf Herzig, unpublished; (based on BDSC #5188)
	RKF1037	P{ry ^{+t7.2} =hsFLP}3F, <i>y</i> [*] <i>w</i> [*] ; <i>D</i> ³ /TM3, <i>Sb</i> ¹ , P{Ubx-lacZ}	Alf Herzig; unpublished
	RKF1038	<i>w</i> [*] ; P{ry ^{+t7.2} =neoFRT}82B <i>plin1</i> ¹	this study
<i>HsPLIN1</i> effector	RKF571	<i>w</i> [*] ; P{w[+mC]UAS-HsPLIN1}/CyO-hb-beta-gal float	this study
<i>plin1</i> ⁻ <i>HsPLIN1</i> effector	RKF1027	<i>w</i> [*] ; P{w ^{+mC} UAS-HsPLIN1}/CyO-hb-beta-gal float; <i>plin1</i> ¹	this study
<i>plin1</i> ⁻ <i>plin2</i> ::EGFP effector	RKF982	<i>w</i> [*] ; P{w ^{+mC} ;UAS- <i>plin2</i> ::EGFP}/CyO float; <i>plin1</i> ¹	this study
<i>plin1</i> ⁻ <i>plin2</i> effector	RKF1039	<i>w</i> [*] ; P{w ^{+mC} UAS- <i>plin2</i> }; <i>plin1</i> ¹	this study
<i>plin2</i> ⁻	RKF610	<i>y</i> [*] <i>plin2</i> ⁵¹ / FM7i; P{w ^{+mC} =ActGFP}JMR3 or <i>hom</i> or <i>Dp(1;Y)</i> <i>y</i> ⁺	(Grönke et al., 2003)
<i>plin1</i> ⁻ <i>plin2</i> ⁻	RKF989	<i>y</i> [*] <i>plin2</i> ⁵¹ / FM7i, P{w ^{+mC} =ActGFP}JMR3 float ; <i>plin1</i> ¹	this study
	RKF1014	<i>y</i> [*] float. <i>w</i> [*] ; +/+; M{3xP3-RFPattP}zh86Fb <i>plin1</i> ¹ ; M{3xP3-RFP;3xP3-EGFP <i>vas-φC31</i> }zh102D	this study
<i>plin1</i> ⁻ <i>bmm</i> ⁻ AKH effector	RKF777	<i>w</i> [*] ; P{UAS-dAKH}; <i>bmm</i> ¹ , <i>plin1</i> ¹ / TM3 <i>Sb</i> ¹ <i>e</i> ¹ float.	this study
<i>plin1</i> ⁻ <i>bmm</i> ⁻ fat body driver	RKF967	<i>w</i> [*] ; P{w[+mW.hs]=GawB}FB+SNS ; <i>bmm</i> ¹ , <i>plin1</i> ¹ / TM6C, <i>Sb</i> ¹ <i>Tb</i> ¹ float.	this study
<i>w</i> (control)		<i>w</i> ¹¹¹⁸	(Grönke et al., 2009)

The fly stock *plin1*^{G4304} carrying an EP-element integration between pos. -508/9 relative to the putative PLIN1 start site (at 3R 19590035) was used to generate the precise excision line *plin1*^{rev} and the *plin1* mutant alleles *plin1*¹ and *plin1*² by a conventional P-element mobilization scheme. *plin1*¹ and *plin1*² mutant alleles carry deletions from pos. -509 to +82 and -509 to +399 relative to the putative PLIN1 start site deleting amino acid pos. 1-28 and pos. 1-133, respectively. Note that both *plin1* mutant alleles carry residual EP-element sequences (2.2kbp in *plin1*¹ and 709bp in *plin1*²). Precise mobilization provided genetically matched control flies *plin1*^{rev}, referred to as *plin1*⁺.

Immunohistochemistry and whole mount *in situ* hybridization

Rabbit anti-PLIN-1 antiserum was raised using a bacterially expressed part of the PLIN1 protein representing amino acid interval 133 to 405 of the PLIN1-PC isoform. Immunohistochemistry on *Drosophila* embryos and larval tissue was performed as described (Grönke et al., 2003) using antibodies/antisera at the following dilutions: rabbit anti-PLIN1, (dil. 1:2000; this work), biotinylated anti-rabbit (dil. 1:500) using the Vectastain ABC kit (www.vectorlabs.com) and anti-rabbit Alexa488/Alexa568 (dil. 1:500; Pierce/Molecular Probes), rat anti-PLIN2 (dil. 1:2000; Teixeira et al., 2003), anti-rat Alexa488 (1:500; Pierce/Molecular Probes), rabbit anti-HsPLIN1a ("PREK"; dil. 1:2000; Souza et al., 1998) combined with anti-rabbit Alexa568 (dil. 1:500; Pierce/Molecular Probes).

Whole mount *in situ* hybridization on embryos was performed as described (Grönke et al., 2003) using *plin1* and *disembodied* (*dib*) probes labeled with fluorescein and DIG RNA labeling mixes (www.roche-applied-science.com), respectively. Probes were detected using the TSA Cyanine 3 system (www.perkinelmer.de) combined with anti-DIG POD and anti-fluorescein POD antibodies (www.roche-applied-science.com) and Cyanine 2 streptavidine.

For double fluorescent *in situ* hybridizations on imaginal discs, larvae were cut at approximately two thirds of the length and inverted in ice cold PBS. Following a 20 min fixation in RNA fixative: PBS (1:1) the specimen were washed with PBT and processed for the *in situ* hybridizations according to the embryo *in situ* RNA hybridization protocol described (Löhr et al., 2009; Supplement) with *plin1* and *plin2* probes labeled with fluorescein and DIG RNA labeling mixes (www.roche-applied-science.com), respectively.

Physiological assays

Food intake was determined with a modified CAFE system using low sugar (1% sucrose/5% yeast extract) and high sugar (10% sucrose/5% yeast extract) liquid food and caloric food composition calculated as described (Ja et al., 2007). Fat (glyceride) content measurements and starvation assays were performed as described in (Grönke et al., 2003). For precise comparison of the *plin1⁻* and *plin1⁺* fly glyceride content during preimaginal ontogenesis, embryo collections of both genotypes were mixed in equal amounts and raised in the same food vial. Genotypes were separated at migratory third instar larval stage using the *plin1⁻* lipid droplet phenotype as diagnostic marker. Locomotor activity of flies on complex food (see above) was assayed using TriKinetics DAM2 systems (www.trikinetics.com). Average circadian and cumulative locomotor activity of 32 *plin1⁺* and *plin1⁻* male flies each were monitored from hatching to day 6 under 12h:12h LD conditions at 25°C.

Semi-quantitative Western blot analysis

Western Blots were carried out as described in the main text with three lanes per sample. Equal amounts of total protein were loaded based on BCA protein measurements as well as housekeeping gene signal (β -Tubulin). Images were acquired with a Fuji LAS-1000 imaging system equipped with an Intelligent Dark Box II with equally sized “regions of interest” delimiting detected signals. Quantifiable images in the Fuji image file format were subsequently analyzed with the Fuji ImageGauge software. Triplicate signals were averaged and tested for statistically significant changes using a two-tailed t-test with unequal variance in Microsoft Excel.

Molecular biology

Quantitative RT-PCR analysis was performed as described in (Grönke et al., 2009). In brief, flies were collected and snap frozen in liquid nitrogen. Total RNA was extracted with the RNeasy mini kit (www.qiagen.com) according to the manufacturer’s instructions. About 300-700ng of total RNA were used for cDNA synthesis with the QuantiTect Reverse Transcription Kit (www.qiagen.com). Serial cDNA dilutions were used to characterize primers in real-time PCR reactions with the FAST Sybr Green Master Mix (www.appliedbiosystems.com) according to the manufacturer’s instructions. Reactions were run in 96-well plates in a StepOnePlus System (www.appliedbiosystems.com) and analyzed with the StepOne Software (Version 2.1) with two housekeeping genes (*Actin 5c* and *Ribosomal protein L32*) as internal controls. mRNA quantifications are shown with 95% confidence intervals. The following primers were used:

Detected gene	Sequence / Identity	Reference
<i>brummer</i>	QT00964460	www.qiagen.com
<i>Act5c</i>	forward: CTGTGCTCTCGCTGTACGC reverse: GATCCAGACGCAGGATGGC	This study
<i>plin1</i>	forward (SGO339): GGCGATCCACGTGCTCTTC reverse (SGO340): GAGATAGACCCACAGTTCCTTG	This study
<i>RpL32</i>	QT00985677	www.qiagen.com

In silico methods

The following sequences were used to construct the phylogenetic tree shown in Figure 1A: *Drosophila melanogaster* LSD-1/PLIN1; *Drosophila melanogaster* LSD-2/PLIN2; *Apis mellifera* GB15498/PLIN1; *Apis mellifera* GB14434/PLIN2; *Apis mellifera* LOC413975/PLIN3; *Aedes aegypti* ABF18439.1/PLIN1; *Aedes aegypti* XP_001658058.1/PLIN2; *Anopheles gambiae* AGAP002890-PA/PLIN1; *Anopheles gambiae* AGAP000167/PLIN2; *Tribolium castaneum* XP_966587/PLIN1; *Tribolium castaneum* XP_976120/PLIN2; *Culex quinquefasciatus* CpipJ_CPIJ003879/PLIN1;

Culex quinquefasciatus CpipJ_CPIJ018160/PLIN2; *Xenopus laevis* Fatvg/PLIN1; *Xenopus laevis* NP_001079660/PLIN2; *Metarhizium anisopliae* ABI18161.1/PLIN1; *Homo sapiens* NP_002657 Perilipin/PLIN1; *Homo sapiens* NP_001113.2 ADRP/PLIN2; *Homo sapiens* NP_005808 Tip47/PLIN3; *Homo sapiens* NP_001073869.1 S3-12/PLIN4; *Homo sapiens* NP_001013728.2 LDSP5/PLIN5.

For the alignment shown in Supplemental Figure 1, amino acid identities were colored with the Jalview tool (<http://www.jalview.org/webstart/jalview.jnlp>) and Phosphosites were introduced in Adobe Illustrator CS3. Phosphosites were either predicted on a global scale with the NetPhos 2.0 tool and standard settings (<http://www.cbs.dtu.dk/services/NetPhos/>) or Protein Kinase A-specific phosphosites were identified with the NetPhosK 1.0 tool and standard settings (<http://www.cbs.dtu.dk/services/NetPhosK>).

NanoLC-ESI and -MALDI mass spectrometry

Lipid droplet-associated proteins were enriched by fat cake preparation. Briefly, fat body cells from 100 immature adult male *plin1*⁺ flies were collected in water supplemented with protease and phosphatase inhibitors (www.roche-applied-science.com; www.sigmaaldrich.com) by manually opening the abdomina and lipid droplets were released by freeze-thaw cycles in liquid nitrogen and by vortexing. Fat cake was separated from the debris by slow speed centrifugation (30 min 2500 rpm) and fat cake proteins precipitated by methanol/chloroform delipidation/precipitation. Proteins were separated on a 12% SDS-PAGE and stained with GelCode Blue (www.piercenet.com). The gel area containing PLIN1 was cut out, reduced with 50 mM DTT for 1 h, alkylated for 1 h with 100 mM IAA and in-gel digested with modified trypsin (www.promega.com) overnight, all at 37°C. Phosphopeptides were enriched by titanium dioxide (TiO₂, www.glsciences.com) as described (Larsen et al., 2005). In brief, aliquots of peptides were dissolved with 20 µl of 200 mg 2,5-dihydroxybenzoic acid (DHB, www.sigmaaldrich.com) in 80% ACN, 5% TFA and loaded onto TiO₂ column. The column was washed 3 times with 20 µl of 200 mg DHB in 80% ACN, 5% TFA and 5 times with 20 µl 80% ACN, 5% TFA. Bound peptides were eluted 3 times with 20 µl of 0.3N NH₄OH, pH≥10.5 and subsequently evaporated with a SpeedVac for further MS analysis. Enriched tryptic peptides were first loaded at a flow rate of 10 µl/min onto an in-house packed C18 pre-column (1.5 cm, 360 µm o.d., 150 µm i.d., Nucleosil 100-5 C18, www.mn-net.com). The retained peptides were then eluted and separated on an analytical C18 column (20 cm, 360 µm o.d., 75 µm i.d., Nucleosil 100-5 C18) at a flow rate of 300 nL/min, with a 60 min gradient from 7.5 to 37.5% ACN in 0.1% formic acid using an Agilent 1100 nano-flow LC system (www.home.agilent.com), coupling with Z-spray source for ESI-MS and -MS/MS (Waters/Micromass Q-ToF Ultima™ API mass spectrometer, Milford, MA). In data dependent acquisition, 1 s survey scans were run over the mass range m/z 350 to 1600. A maximum of three concurrent MS/MS acquisitions were triggered for 2+, 3+, and 4+ charged precursors detected at intensity above 15 counts, after 3 s of acquisition, the system switched back to survey scan mode. All spectra were searched MASCOT v2.2 against the NCBI nr database limited to

Drosophila with criteria-peptide mass tolerance, 50ppm; MS/MS ion mass tolerance, 0.25 Da; allow up to two missed cleavage; variable modifications considered were phosphorylation of serine, threonine and tyrosine, methionine oxidation and cysteine carboxyamidomethylation. All phosphorylated sites were examined manually by the presence of a 69 Da between fragment ions for phosphoserine and an 83 Da for phosphothreonine.

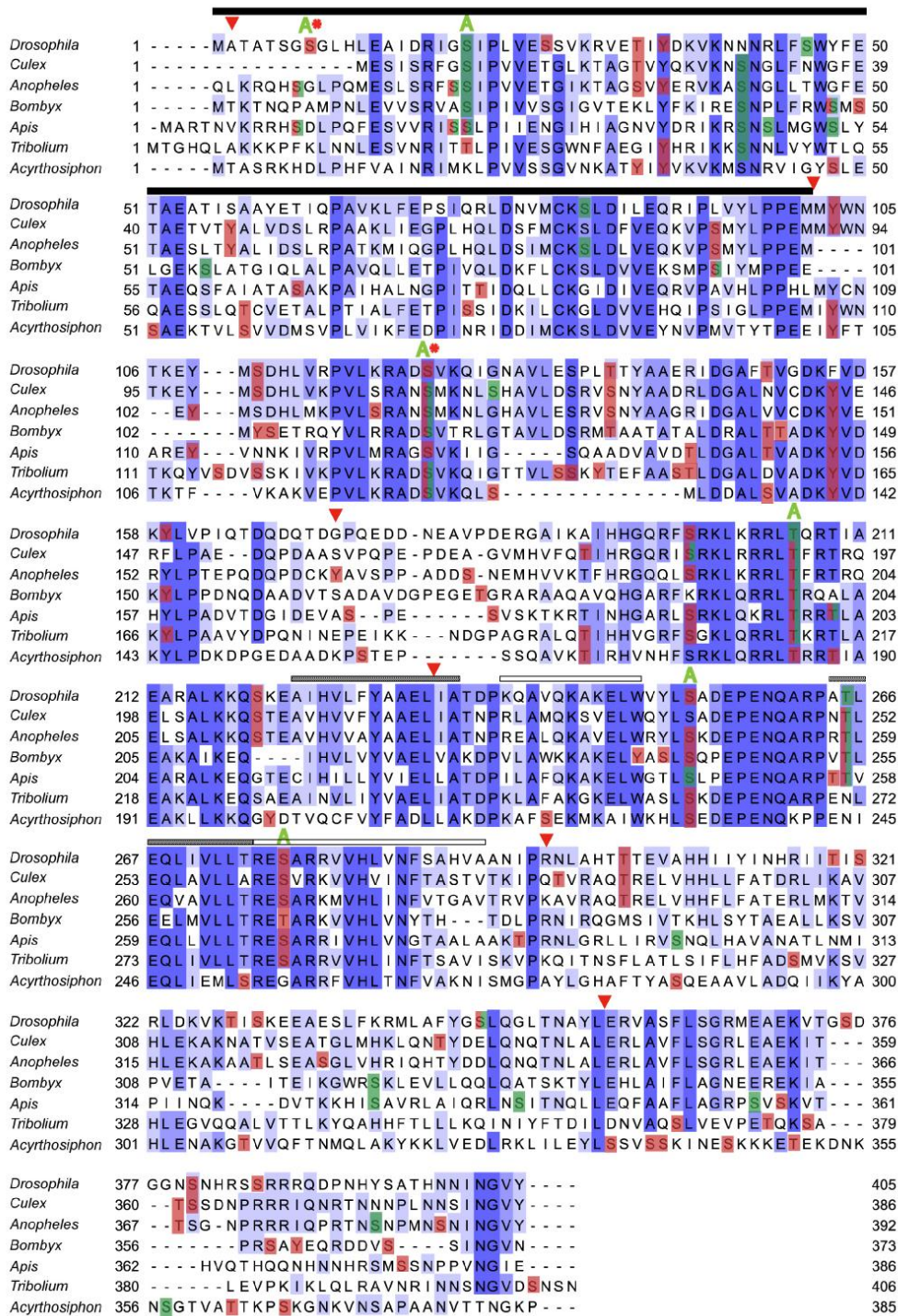


Figure S1. Sequence Alignment of Insect PERILIPIN1 Family Members, Related to Figure 1. Intensity of blue shading reflects degree of amino acid conservation at corresponding amino acid positions among PLIN1 proteins of the fruit fly *Drosophila melanogaster*, the two mosquito species *Culex pipiens* and *Anopheles gambiae*, the

silkworm *Bombyx mori*, the honeybee *Apis mellifera*, the beetle *Tribolium castaneum* and the pea aphid *Acyrtosiphon pisum*. Insect PLIN1 proteins consist of the N-terminal PAT domain (black bar) followed by two sequence-conserved regions connected by a variable linker and an evolutionarily less conserved C-terminus. Note that the second conserved region covers the predicted hydrophobic helices (hatched boxes) and amphipatic helices with high hydrophobic moment (open boxes) proposed to act as lipid interaction domains (Arrese et al., 2008). Amino acids shaded in brown or green represent *in silico* predicted S/T phosphorylation sites and Protein kinase A phosphorylation sites, respectively. Predicted or *in vivo* confirmed (red star) phosphorylation sites substituted by alanine in *Drosophila* PLIN1^{ΔH} are indicated by green "A". Red triangles map the *Drosophila plin1* splice sites on fruit fly PLIN1.

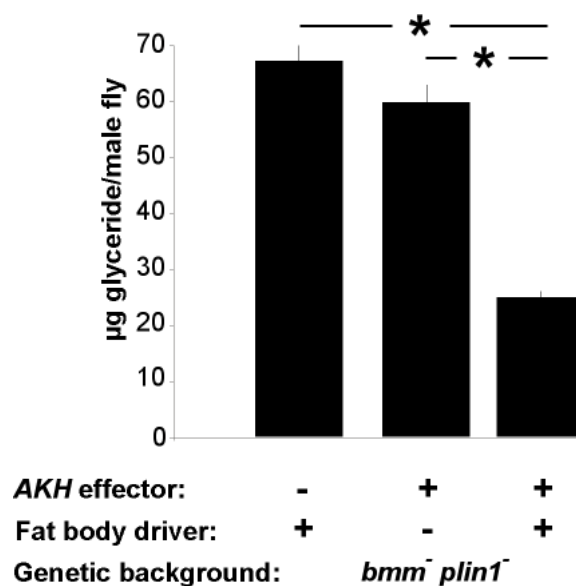
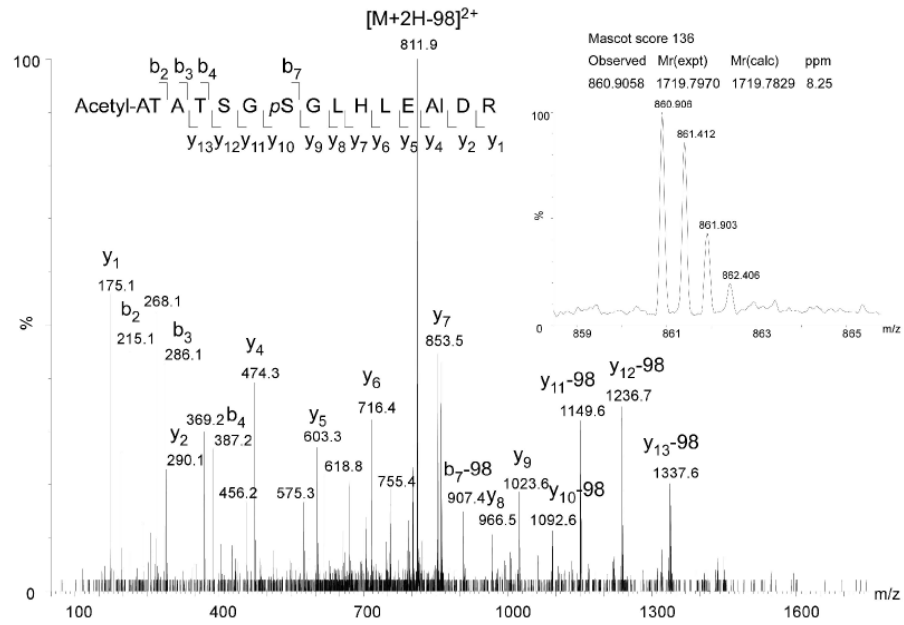


Figure S2. AKH-Induced Leanness by a Lipolysis-Independent Mechanism, Related to Figure 4. AKH overexpression reverts obesity of fat mobilization-incompetent *bmm⁻ plin1⁻* double mutants supporting a function of AKH in lipogenesis repression. Shown is a representative experiment based on triplicate measurements involving a total of 24 male flies per genotype. Error bars represent STDEVP; * p<0.05.

A Phosphoserine at PLIN1 amino acid position 8:



B Phosphoserine at PLIN1 amino acid position 124:

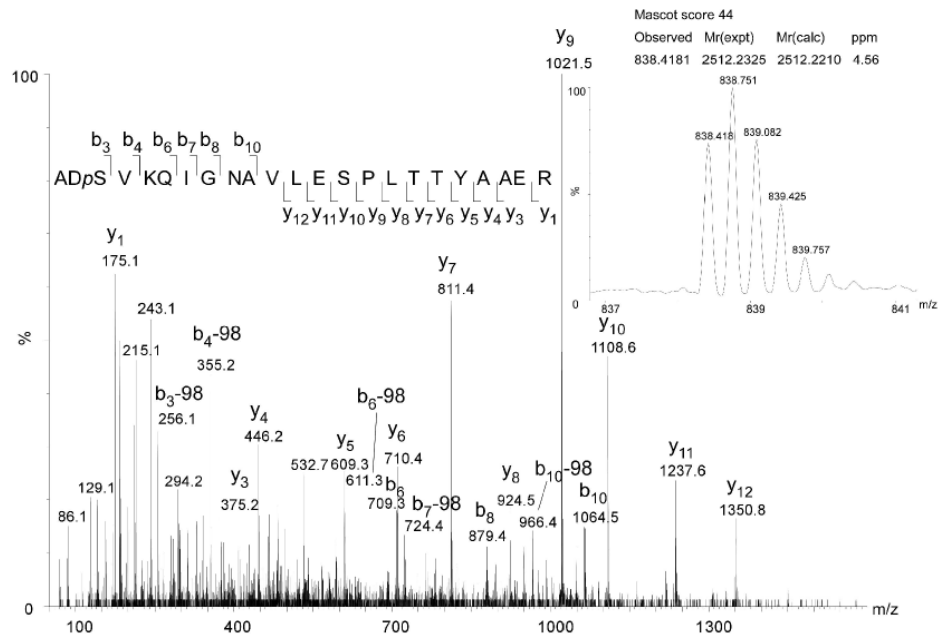


Figure S3. Related to Figure 4 and Figure S1. MS/MS spectrum of phosphorylated PLIN1 peptides acetyl-ATATSGpSGLHLEAIDR (A) and ADpSVKQIGNAVLESPLTTYAAER (B) at m/z 860.9 and 838.4, respectively.

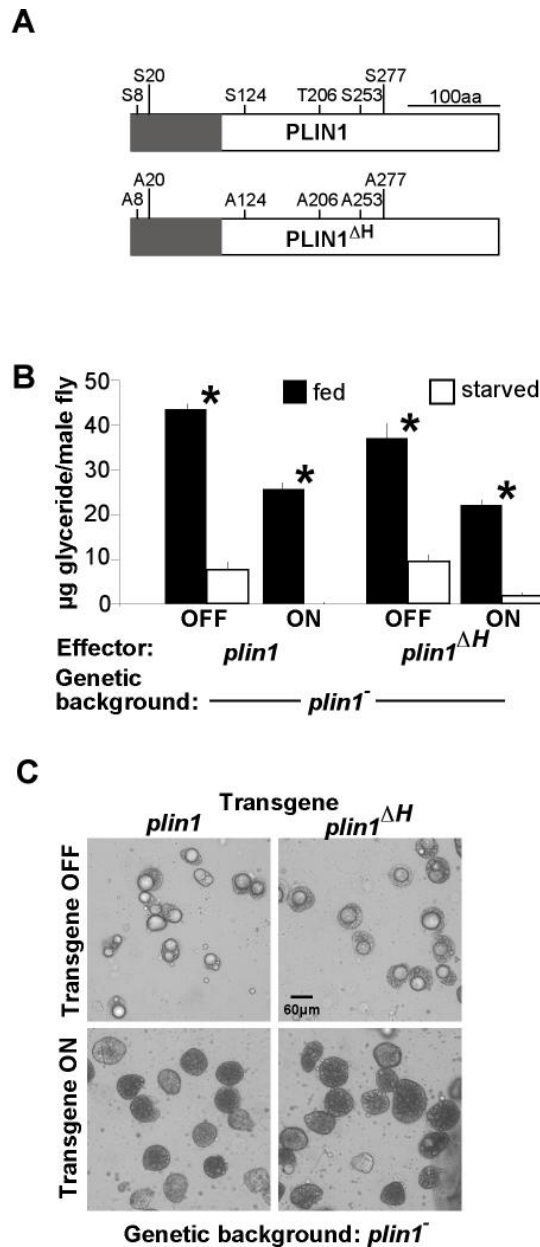


Figure S4. Phosphorylation Site Mutant PLIN1 Is Active *In Vivo*, Related to Figure 4 and Figure S1. (A) Schematic representation of wild type PLIN1 and PLIN1^{ΔH} a mutant variant, which carries alanine replacements of six confirmed or predicted serine/threonine phosphorylation sites (N-terminal PAT-domain in grey). Lipid storage (B) and structural phenotype (C) of *plin1* mutants rescued by a *plin1* or *plin1*^{ΔH} transgene. Pictures in (C) show brightfield images of fat body cells from immature adult male *plin1*⁻ flies with an inactive (OFF) or active (ON) *plin1* or *plin1*^{ΔH} transgene. Shown in (B) is a representative experiment based on triplicate measurements involving a total of 24 male flies per genotype. Error bars represent STDEVP; * $p < 0.05$.

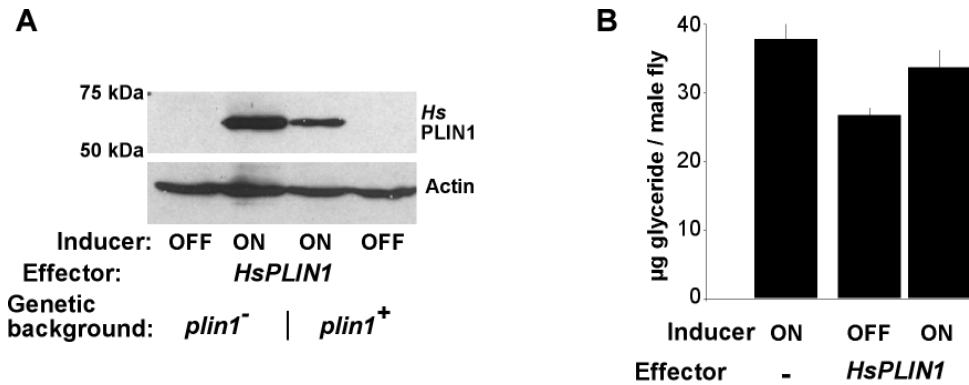


Figure S5. Related to Figure 6. Conditional expression of human Perilipin1 (*HsPLIN1*) in the fat body of transgenic *plin1*⁺ or *plin1*⁻ flies detected by Western blot analysis (**A**) does not influence the body fat content of *plin1*⁺ flies (**B**) or *plin1*⁻ flies (see Figure 6B). Shown in (**B**) is a representative experiment based on triplicate measurements involving a total of 24 male flies per genotype. Error bars represent STDEVP.

Supplemental References

Arrese, E. L., Rivera, L., Hamada, M., Mirza, S., Hartson, S. D., Weintraub, S., and Soulages, J. L. (2008b). Function and structure of lipid storage droplet protein 1 studied in lipoprotein complexes. *Arch. Biochem. and Biophys.* *473*, 42-47.

Bischof, J., Maeda, R. K., Hediger, M., Karch, F., and Basler, K. (2007). An optimized transgenesis system for *Drosophila* using germ-line-specific phiC31 integrases. *Proc. Natl. Acad. Sci. U.S.A.* *104*, 3312-3317.

Brand, A., and Perrimon, N. (1993). Targeted gene expression as a means of altering cell fates and generating dominant phenotypes. *Development* *118*, 401-415.

Buszczak, M., Lu, X., Segraves, W. A., Chang, T. Y., and Cooley, L. (2002). Mutations in the *midway* gene disrupt a *Drosophila* acyl coenzyme A: diacylglycerol acyltransferase. *Genetics* *160*, 1511-1518.

Dietzl, G., Chen, D., Schnorrer, F., Su, K.-C., Barinova, Y., Fellner, M., Gasser, B., Kinsey, K., Oppel, S., Scheiblauer, S., *et al.* (2007). A genome-wide transgenic RNAi library for conditional gene inactivation in *Drosophila*. *Nature* *448*, 151-156.

Grönke, S., Beller, M., Fellert, S., Ramakrishnan, H., Jäckle, H., and Kühnlein, R. P. (2003). Control of fat storage by a *Drosophila* PAT domain protein. *Curr. Biol.* *13*, 603-606.

Grönke, S., Bickmeyer, I., Wunderlich, R., Jäckle, H., and Kühnlein, R. (2009). curled Encodes the *Drosophila* Homolog of the Vertebrate Circadian Deadenylase Nocturnin. *Genetics* *183*, 219-232.

Grönke, S., Mildner, A., Fellert, S., Tennagels, N., Petry, S., Müller, G., Jäckle, H., and Kühnlein, R. (2005). Brummer lipase is an evolutionary conserved fat storage regulator in *Drosophila*. *Cell Metab.* *1*, 323-330.

Grönke, S., Müller, G., Hirsch, J., Fellert, S., Andreou, A., Haase, T., Jäckle, H., and Kühnlein, R. P. (2007). Dual lipolytic control of body fat storage and mobilization in *Drosophila*. *PLoS Biol.* *5*, e137.

Ja, W., Carvalho, G., Mak, E., de la Rosa, N., Fang, A., Liang, J., Brummel, T., and Benzer, S. (2007). Prandiology of *Drosophila* and the CAFE assay. *Proc. Natl. Acad. Sci. U.S.A.* *104*, 8253-8256.

Kiger, J. A., Eklund, J. L., Younger, S. H., and O'Kane, C. J. (1999). Transgenic inhibitors identify two roles for protein kinase A in *Drosophila* development. *Genetics* 152, 281-290.

Larsen, M. R., Thingholm, T. E., Jensen, O. N., Roepstorff, P., and Jørgensen, T. J. D. (2005). Highly selective enrichment of phosphorylated peptides from peptide mixtures using titanium dioxide microcolumns. *Mol. Cell. Proteomics* 4, 873-886.

Löhr, U., Chung, H.-R., Beller, M., and Jäckle, H. (2009). Antagonistic action of Bicoid and the repressor Capicua determines the spatial limits of *Drosophila* head gene expression domains. *Proc. Natl. Acad. Sci. U.S.A.* 106, 21695-21700.

McGuire, S., Le, P., Osborn, A., Matsumoto, K., and Davis, R. (2003). Spatiotemporal rescue of memory dysfunction in *Drosophila*. *Science* 302, 1765-1768.

Souza, S., de Vargas, L., Yamamoto, M., Lien, P., Franciosa, M., Moss, L., and Greenberg, A. (1998). Overexpression of perilipin A and B blocks the ability of tumor necrosis factor alpha to increase lipolysis in 3T3-L1 adipocytes. *J. Biol. Chem.* 273, 24665-24669.

Teixeira, L., Rabouille C., Rorth, P., Ephrussi, A., and Vanzo, N.F. (2003). *Drosophila* Perilipin/ADRP homologue Lsd2 regulates lipid metabolism. *Mech. Dev.* 120, 1071-1081.

Vorbrüggen, G., and Jäckle, H. (1997). Epidermal muscle attachment site-specific target gene expression and interference with myotube guidance in response to ectopic stripe expression in the developing *Drosophila* epidermis. *Proc. Natl. Acad. Sci. U.S.A.* 94, 8606-8611.